Hindawi
Advances in Condensed Matter Physics
Volume 2024, Article ID 9911970, 9 pages
https://doi.org/10.1155/2024/9911970

Research Article

Effect of Tunable Dielectric Core on Optical Bistability in Cylindrical Core–Shell Nanocomposites

Shewa Getachew

Department of Physics, Wolkite University, P. O. Box 07, Wolkite, Ethiopia

Correspondence should be addressed to Shewa Getachew; shewa.getachew@wku.edu.et

Received 10 November 2023; Revised 29 February 2024; Accepted 13 March 2024; Published 26 March 2024

Academic Editor: Junjie Li

In this paper, the effect of a tunable dielectric core on local field enhancement, induced optical bistability, and the optical bistability domain in cylindrical core–shell nanoparticle composites are studied. The local field enhancement factor increases significantly at two resonant frequencies. The results demonstrate that the local field enhancement factor in the cylindrical core–shell nanoparticle increases when the natural attribute of the dielectric function of the dielectric core is varied by adding a dielectric function to it. Furthermore, we demonstrated that the magnitude of the imaginary part of the active dielectric core increases as the onset and offset input intensities increase. This indicates that the optical bistability or threshold width range widens as the imaginary part of the dielectric function of the dielectric core increases, thereby enlarging the threshold domain to improve system activation.

1. Introduction

Enhancing the local electric field within core–shell nanoparticles is crucial for the development of nonlinear optical effects. The differences in dielectric characteristics between the host matrix and the composite, as well as the nanoscale sizes and shapes of the metal–dielectric composite, significantly contribute to this enhancement [1–3]. When the metal fraction (p) and dielectric of the host matrix increase, the amplitude of the local field enhancement (LFE) factor also increases in both passive and active dielectric cores. This indicates that when the radius of the core increases, i.e., when the p value decreases, the enhancement factor of cylindrical core–shell nanocomposites decreases, leading to a smaller amplitude [4]. Optical-induced bistability (OIB), characterized by a single input field resulting in two different values of the local field intensity, is a significant nonlinear optical effect observed in plasmonic nanocomposites [5, 6]. Its potential applications in optoelectronics and logic elements make it an area of considerable interest [7].

In addition, the local electric field in these composites is significantly strengthened by surface plasmon (SP) resonance, which arises from localized surface plasmonics. These fields can be generated by laser light; however, abnormal amplification of the local field occurs when the incident electromagnetic wave frequency approaches the metal's SP frequency [8]. Induced optical bistability (IOB) has shown significant theoretical and experimental progress, but due to its numerous potential applications, further research is imperative [9, 10].

Mal'nev and Shewamare [11] investigated the LFE at the focal point of spherical nanoinclusions in a linear dielectric host matrix. Their research highlighted the superior performance of LFE when the frequency of the incident electromagnetic wave approaches the SP frequency of the metal component of the inclusions. By altering the thickness of the metal within coated inclusions, researchers can identify the maximum value of the enhancement factor. The significance of the enhancement factor increases for both dielectric-coated metal inclusions with thin metal cores and those with thick metal covers [12].

This work proposes the alternative method for tuning the dielectric function of the core in cylindrical core–shell nanoparticles implanted within a linear host matrix, thereby enhancing the local field, optical bistability, and its domain within metal–dielectric composites. The optical density of the core–shell nanocomposite structure is increased by introducing an additional imaginary component to the dielectric core, which enhances the interactions between light and the

core–shell nanocomposite. This increase in optical density widens the threshold for optically induced bistability and augments the LFE factor within the composite.

The remainder of the paper is organized as follows: Section 2 discusses the enhancement of the local field in cylindrical core–shell nanoparticles. Section 3 presents numerical results and discussions, while Section 4 provides a summary and conclusion.

2. The Enhancement of Local Field in Cylindrical Core–Shell Nanoparticles

In classical electrodynamics, the Laplace equation (i.e., $\nabla^2\phi = 0$) in a cylindrical coordinate system has a general form given by the following equation [13]:

$$\frac{\partial^2\phi}{\partial r^2} + \frac{1}{r}\frac{\partial\phi}{\partial r} + \frac{1}{r^2}\frac{\partial\phi}{\partial\theta^2} + \frac{\partial\phi}{\partial z^2} = 0. \tag{1}$$

In a cylindrical coordinate system, the potential is 2D, and its choice is not dependent on the z-axis. In this case, Equation (1) can be reduced to the following form:

$$\frac{\partial^2\phi}{\partial r^2} + \frac{1}{\partial r}\frac{\partial\phi}{\partial r} + \frac{1}{r^2}\frac{\partial}{\partial\theta^2} = 0. \tag{2}$$

The solution of Equation (2) can provide the potential distribution in various regions of a composite material consisting of metal-coated dielectric-core cylindrical nanoinclusions embedded in a linear dielectric host matrix, as described in Abbo et al.'s [14] study:

$$\begin{aligned} \phi_d &= -E_h A r\cos\theta, && r \le r_1 \\ \phi_m &= -E_h\left(Br - \frac{C}{r}\right)\cos\theta, && r_1 \le r \le r_2 \\ \phi_h &= -E_h\left(r - \frac{D}{r}\right)\cos\theta, && r \ge r_2, \end{aligned} \tag{3}$$

where ϕ_d, ϕ_m, and ϕ_h are potentials in the dielectric core, metallic shell, and the dielectric host matrix, respectively, E_h is the applied field (for the cylindrical inclusion, it is perpendicular to its axis), r_1 and r_2 are the radii of the dielectric core and the metal shell, respectively, and A, B, C, and D are unknown coefficients. We can calculate the enhancement factor A using this. The unknown coefficients can be obtained from the electrostatic boundary conditions, which means using dielectric boundary conditions (DBC). These boundary conditions state that at interfaces between different dielectric materials, DBC are utilized to ensure continuity of the electric displacement and the normal component of the electric field. Under the long-wave approximation, where the wavelength of the incident electromagnetic wave is greater than the size of the particle, we can use the following electrostatic boundary conditions to determine the values of the coefficients [15] (Figure 1).

From the continuity conditions of the electric potential and the displacement vector at the interface between the

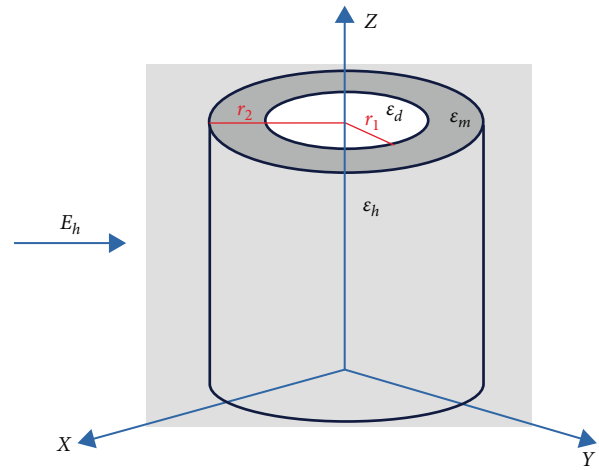

Figure 1: The schematic figure shows a core–shell nanostructure consisting of a cylindrical dielectric particle with dielectric constant ε_d, coated by a metal shell with dielectric function ε_m, embedded in a host matrix with dielectric function ε_h.

dielectric core, metal, and host matrix, we derive the system of linear algebraic equations for the unknown coefficients:

$$A = B - \frac{C}{r_1^2}, \tag{4}$$

$$B - \frac{C}{r_2^2} = 1 - \frac{D}{r_2^2}. \tag{5}$$

From the continuity condition of the displacement vector:

$$A\varepsilon_d = \varepsilon_m\left(B + \frac{C}{r_1^2}\right), \tag{6}$$

$$\varepsilon_m\left(B + \frac{C}{r_2^2}\right) = \varepsilon_h\left(1 + \frac{D}{r_2^2}\right). \tag{7}$$

The expressions for the unknown constants are determined in terms of the dielectric constants of the host (ε_h), metal cover (ε_m), and dielectric core (ε_d).

Substituting Equation (4) into Equation (6), we obtain the following equation:

$$B = \left(\frac{\varepsilon_m + \varepsilon_d}{\varepsilon_d - \varepsilon_m}\right)\frac{C}{r_1^2}. \tag{8}$$

Putting Equation (8) into Equation (5), we have the following equation:

$$\frac{C}{r_1^2}\left(\frac{\varepsilon_m(2-p) + p\varepsilon_d}{\varepsilon_d - \varepsilon_m}\right) = 1 - \frac{D}{r_2^2}. \tag{9}$$

Substituting Equation (8) into Equation (7), we obtain the following equation:

$$\frac{C}{r_1^2}\left(\frac{\varepsilon_d\varepsilon_m(2-p)+p\varepsilon_m^2}{\varepsilon_d-\varepsilon_m}\right)=\varepsilon_h+\varepsilon_h\frac{D}{r_2^2}. \tag{10}$$

Multiplying Equation (9) by ε_h, we have the following equation:

$$\frac{C}{r_1^2}\left(\frac{(2-p)\varepsilon_m\varepsilon_h+p\varepsilon_d\varepsilon_h}{\varepsilon_d-\varepsilon_m}\right)=\varepsilon_h-\varepsilon_h\frac{D}{r_2^2}. \tag{11}$$

By adding Equation (11) with Equation (10), we get the following equation:

$$\frac{C}{r_1^2}=\frac{2\varepsilon_h(\varepsilon_d-\varepsilon_m)}{p\nabla}, \tag{12}$$

where

$$\nabla=\varepsilon_m^2+q\varepsilon_m+\varepsilon_d\varepsilon_h, \tag{13}$$

$$q=\left(\frac{2}{p}-1\right)\varepsilon_h+\left(\frac{2}{p}-1\right)\varepsilon_d, \tag{14}$$

$$p=1-\left(\frac{r_1}{r_2}\right)^3. \tag{15}$$

The dielectric function of the core, denoted as ε_d, is chosen to be a complex value that is independent of frequency. The dielectric constant of the host medium, denoted as ε_h, is real, while the dielectric function of the metal cover, denoted as ε_m, is chosen to follow the Drude form.

Substituting Equation (12) into Equation (8), we obtain the following equation:

$$B=\frac{2\varepsilon_h(\varepsilon_d+\varepsilon_m)}{p\nabla}. \tag{16}$$

Substituting Equations (12) and (16) into Equation (4), we have the following equation:

$$A=\frac{4\varepsilon_h\varepsilon_m}{p\nabla}. \tag{17}$$

Equation (17) indicates the LFE factor of cylindrical core–shell nanoparticles. Recall that the dielectric function of the dielectric inclusion is given by the following equation:

$$\begin{aligned}\varepsilon_m&=\varepsilon_\infty-\frac{1}{z(z+iz)}\\ \varepsilon_m'&=\varepsilon_\infty'-\frac{1}{z^2+\gamma^2}\\ \varepsilon_m''&=\varepsilon_\infty''+\frac{\gamma}{z(z^2+\gamma^2)},\end{aligned} \tag{18}$$

where ε_m' and ε_m'' are the real and imaginary parts of ε_m, respectively. Here, $z=\omega/\omega_p$ represents the dimensionless frequency, where ω is the frequency of the incident radiation, ω_p is the plasma frequency of the inclusion metal part, ν is the electron collision frequency, and $\gamma=\nu/\omega_p$. By squaring the enhancement factor, we obtain the following equation:

$$|A|^2=\frac{16\varepsilon_h^2}{p^2}\left|\frac{\varepsilon_m}{\nabla}\right|^2, \tag{19}$$

where

$$\begin{aligned}|\varepsilon_m|^2&=|\varepsilon_m'|+|\varepsilon_m''|^2\\ |\nabla|^2&=[\varepsilon_m^2+q\varepsilon_m+\varepsilon_d\varepsilon_h]^2,\\ |\nabla|^2&=[\nabla']^2+[\nabla'']^2\\ \nabla'&=\varepsilon_m'^2-\varepsilon_m''^2+q'\varepsilon_m'-q''\varepsilon_m''+\varepsilon_d'\varepsilon_h\\ \nabla''&=2\varepsilon_d'\varepsilon_m''+q'\varepsilon_m''+q''\varepsilon_m'+\varepsilon_d''\varepsilon_h\\ \varepsilon_d&=\varepsilon_d'+i\varepsilon_d'',\quad q=q'+iq''\\ q'&=\left(\frac{2}{p}-1\right)\varepsilon_d'+\left(\frac{2}{p}-1\right)\varepsilon_h\\ q''&=-\left(\frac{2}{p}-1\right)\varepsilon_d''.\end{aligned} \tag{20}$$

Thus, the LFE factor is determined as follows:

$$|A|^2=\frac{16\varepsilon_h(|\varepsilon_m'|^2+|\varepsilon_m''|^2)}{p^2[|\nabla'|^2+|\nabla''|^2]}. \tag{21}$$

2.1. Induced Optical Bistability in Cylindrical Nanoparticles. SPs are transverse waves that propagate along the interface between a metal surface and a dielectric medium. They are supported by the collective oscillation of free electrons at the metal–dielectric interface, which gives rise to a surface charge density that interacts with the incident electromagnetic field. Specifically, SPs can be sustained in transverse magnetic (TM) modes of propagation, characterized by a magnetic field component perpendicular to the interface. Moreover, the excitation of SPs is highly dependent on the wavelength and incident angle of the incoming radiation. At a certain combination of wavelength and incident angle, known as the resonance condition, the energy of the incident radiation can be efficiently transferred to the SPs. This results in strong electromagnetic field confinement and enhancement near the interface. The formation of SP is due to the electric field of an incoming radiation that induces the formation of a dipole or a polarization of charges on the nanoparticle surface. The local electric field E can be represented in the following form:

$$E=AE_h, \tag{22}$$

where A is the enhancement factor, E is the local field, and E_h is the applied field.

We consider a cylindrical dielectric particle (the core) with a radius of r_1, covered by a metal shell with a radius of r_2. Let the core be a nonlinear dielectric of the Kerr type with a nonlinear dielectric function:

$$\varepsilon_d = \varepsilon_{d0} + \chi|E|^2, \tag{23}$$

where ε_{d0} represents the linear part of the dielectric function, and the Kerr coefficient, denoted as χ and mentioned in Equation (23), represents the nonlinear optical response of the dielectric profile for the core material. It characterizes the strength of this nonlinear response and is crucial for understanding the material's behavior in nonlinear optical processes. Substituting Equation (23) into Equation (13), we obtain the following equation:

$$\nabla = \varepsilon_m^2 + q\varepsilon_m + (\varepsilon_{d0} + \chi|E|^2)\varepsilon_h, \tag{24}$$

Since

$$\begin{aligned} q &= \left(\frac{2}{p} - 1\right)\varepsilon_d + \left(\frac{2}{p} - 1\right)\varepsilon_h \\ q &= \left(\frac{2}{p} - 1\right)(\varepsilon_{d0} + \chi|E|^2) + \left(\frac{2}{p} - 1\right)\varepsilon_h \\ q &= \left(\frac{2}{p} - 1\right)\varepsilon_{d0} + \left(\frac{2}{p} - 1\right)\chi|E|^2 + \left(\frac{2}{p} - 1\right)\varepsilon_h. \end{aligned} \tag{25}$$

Substituting Equation (25) into Equation (24), we obtain the following equation:

$$\begin{aligned} \nabla &= \varepsilon_m^2 + \left[\left(\frac{2}{p} - 1\right)\varepsilon_{d0} + \left(\frac{2}{p} - 1\right)\varepsilon_h\right]\varepsilon_m \\ &\quad + \varepsilon_{d0}\varepsilon_h + \left(\left(\frac{2}{p} - 1\right)\varepsilon_m + \varepsilon_h\right)\chi|E|^2 \\ \nabla &= \nabla_0 + \sigma\chi|E|^2, \end{aligned} \tag{26}$$

where

$$\begin{aligned} \nabla_0 &= \varepsilon_m^2 + \left[\left(\frac{2}{p} - 1\right)\varepsilon_{d0} + \left(\frac{2}{p} - 1\right)\varepsilon_h\right]\varepsilon_m + \varepsilon_{d0}\varepsilon_h \\ q_0 &= \left(\frac{2}{p} - 1\right)\varepsilon_{d0} + \left(\frac{2}{p} - 1\right)\varepsilon_h \\ \sigma &= \left[\left(\frac{2}{p} - 1\right)\varepsilon_m + \varepsilon_h\right]\chi|E|^2 \\ \nabla_0 &= \varepsilon_m^2 + \varepsilon_m q_0 + \varepsilon_{d0}\varepsilon_h \\ \nabla_0 &= \nabla_0' + i\nabla_0'', \quad \varepsilon_{d0} = \varepsilon_d' + i\varepsilon_d'' \\ \sigma &= \sigma' + i\sigma'', \quad q_0 = q_0' + iq_0''. \end{aligned} \tag{27}$$

By substituting the above value for the enhancement factor, we obtain the following equation:

$$|A|^2 = \frac{16}{p^2}\left|\frac{\varepsilon_h\varepsilon_2}{\sigma}\right|^2 \frac{1}{\left|\frac{\nabla_0}{\sigma}\right|^2 + 2Re\left(\frac{\nabla_0}{\sigma}\right)\chi|E|^2 + |\chi|E^{|2|2}|}. \tag{28}$$

By squaring Equation (22) and multiply by χ, we have the following equation:

Table 1: Numerical values of physical quantities [11, 14].

Constants	Values
ε_d'	6.0
ε_h	2.25
ε_∞	4.5
ω_p	1.6×10^{16}
ν	1.68×10^{14}
γ	1.15×10^{-2}

$$\chi|E|^2 = |A|^2\chi|E_h|^2. \tag{29}$$

Substituting Equation (28) into Equation (29), we obtain the following equation:

$$\chi|E|^2 = \frac{16}{p^2}\left|\frac{\varepsilon_h\varepsilon_2}{\sigma}\right|^2 \frac{\chi|E_h|^2}{\left(\frac{\nabla_0}{\sigma}\right)^2 + 2Re\left(\frac{\nabla_0}{\sigma}\right)\chi|E|^2 + |\chi|E^{|2|2}|}. \tag{30}$$

Recall that the modulus of the dielectric function of core–shell nanoinclusion is given by the following equation:

$$\begin{aligned} |\varepsilon_m'|^2 &= |\varepsilon_m'|^2 + |\varepsilon_m''|^2 \\ |\nabla_0|^2 &= |\nabla_0'|^2 + |\nabla_0''|^2 \\ |\sigma|^2 &= |\sigma'| + |\sigma''|^2 \\ \varepsilon_m'' &= \varepsilon_\infty' - \frac{1}{z^2+\gamma^2}, \quad \varepsilon_m'' = \varepsilon_\infty'' + \frac{\gamma}{z(z^2+\gamma^2)} \\ \nabla_0'^2 &= \varepsilon_m'^2 - \varepsilon_m''^2 + q\varepsilon_m' + \varepsilon_d'\varepsilon_h, \quad \nabla_0'' = 2\varepsilon_m'\varepsilon_m'' + q\varepsilon_m'' + \varepsilon_d''\varepsilon_h \\ \sigma' &= \left(\frac{2}{p} - 1\right)\varepsilon_m' + \varepsilon_h, \quad \sigma'' = \left(\frac{2}{p} - 1\right)\varepsilon_m''. \end{aligned} \tag{31}$$

And by obtaining $X = \chi|E|^2$ and $Y = \chi|\varepsilon_h|^2$, the above equation becomes:

$$\eta Y = X^3 + aX^2 + bX, \tag{32}$$

where

$$\eta = \frac{16}{p^2}\left|\frac{\varepsilon_h\varepsilon_2}{\sigma}\right|^2, \quad b = \left|\frac{\nabla_0}{\sigma}\right|^2, \quad a = 2Re\left(\frac{\nabla_0}{\gamma}\right). \tag{33}$$

3. Numerical Results and Discussions

All the numerical values of the dielectric functions of the composite used in this section are taken from references, and Table 1 shows the constant values used in numerical calculations.

3.1. The Enhancement Factor of Cylindrical Core–Shell Nanoparticles of Passive Dielectric Core. Passive dielectric core is a medium that is considered to possess a natural property whereby its dielectric function remains unaffected,

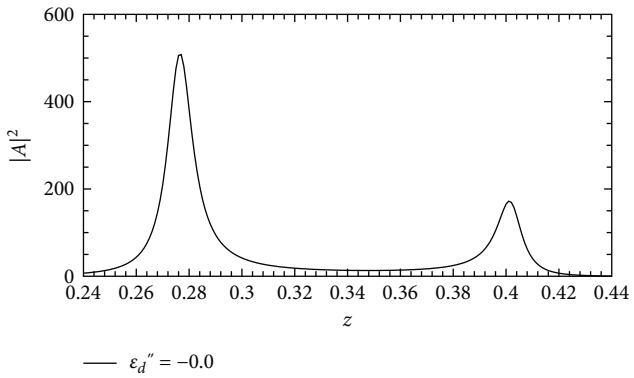

FIGURE 2: The enhancement factor $|A|^2$ for cylindrical core–shell nanoparticles versus z for $\varepsilon_d' = 6$ at metallic fraction of $p = 0.9$. We use the following parameters of the system: $\omega_p = 1.4 \times 10^{16}$, $\nu = 1.68 \times 10^{14}$, $\gamma = 1.15 \times 10^{-2}$, $\varepsilon_\infty' = 4.5$, $\varepsilon_\infty'' = 0$, and $\varepsilon_h = 2.25$.

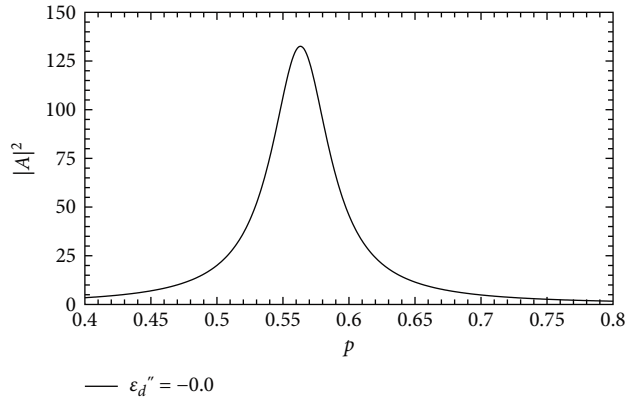

FIGURE 3: Enhancement factor versus metal fraction p of the core–shell nanoparticle with passive dielectric core ($\varepsilon_d'' = 0.0$) at $z = 0.2$, $\varepsilon_d' = 6.0$, and $\varepsilon_h = 2.25$.

as there is no external dielectric function added to it. Therefore, the imaginary part of the dielectric function of the dielectric core is zero ($\varepsilon_d'' = 0$). The plot of the enhancement factor, as stated in Equation (21), for cylindrical core–shell nanoparticles with a passive dielectric core is shown in Figures 2 and 3. The enhancement factor A varies with dimensionless resonant frequency (z), as shown in Figures 2 and 3, $|A|^2$ versus z. Figure 2 shows that the enhancement factor has two peak values at two separate dimensionless resonant frequencies for a composite with metal-coated dielectric cylindrical inclusions. The host dielectric and the dielectric core are interfaced with the metal shell. As a result, at the interfaces between the dielectric host matrix and the dielectric core, the free electrons of the metal fluctuate at various SP frequencies. The enhancement factor significantly increases at these two dimensionless resonant frequencies. Figure 2 depicts two dimensionless resonant frequencies (z). It is possible that the wavelengths presented are normalized to these resonant frequencies. This normalization aids in understanding how the wavelengths interact with the resonant behavior of the system, providing valuable insights into its

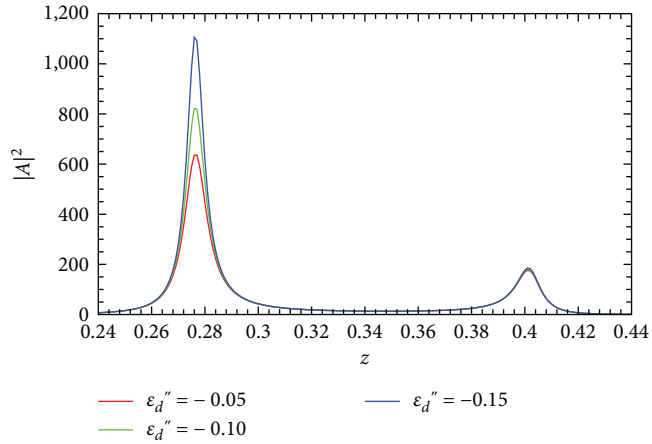

FIGURE 4: The local field enhancement factor $|A|^2$ for cylindrical shell–core nanoparticle versus z with $\varepsilon_d'' = -0.05$ (red line), $\varepsilon_d'' = -0.10$ (green line), and $\varepsilon_d'' = -0.15$ (blue line) in linear host matrix.

optical properties. Figure 3 shows the enhancement factor of nanoparticles with cylindrical core–shell structures separated by a metal layer versus the metal fraction (p), for different distinct values of the dielectric core. This result indicates that for a given resonant frequency, there is only one maximum value of the enhancement factor for a composite containing dielectric cylindrical nanoinclusions coated with metal.

3.2. The Enhancement Factor of Cylindrical Core–Shell Nanoparticles of Active Dielectric Core. The active dielectric core is a medium considered to have a natural property, whereby its imaginary part of the dielectric function is affected by applying an additional dielectric function to it. Therefore, the imaginary part of the dielectric function of the dielectric core is nonzero ($\varepsilon_d'' \neq 0$). The presence of the imaginary dielectric function suggests that the dielectric core has absorbed energy from the incident electromagnetic field, leading to attenuation as the field propagates through the material. The change in the imaginary part of the dielectric function with the field intensity signifies the intensity-dependent absorption characteristics of the material, which could have arisen from various physical mechanisms, such as nonlinear optical processes or material defects. In an active dielectric core, the imaginary part of the dielectric function has a negative sign, indicating that an additional dielectric function is applied to the dielectric core.

Figure 4 shows the LFE factor expressed in Equation (21) for a cylindrical core–shell nanoparticle with an active dielectric core, illustrating different values of ε_d''. In Figure 4, we have observed that there are different maximum values of the LFE factor for various values of the active dielectric core ($\varepsilon_h'' < 0$). When modifying the inherent property of the dielectric function of the core by introducing an additional dielectric function to it, the amplitude of the graph, or $|A|^2$, increases. Therefore, for the active dielectric core ($\varepsilon_d'' < 0$), the LFE factor can be maximized by altering the original

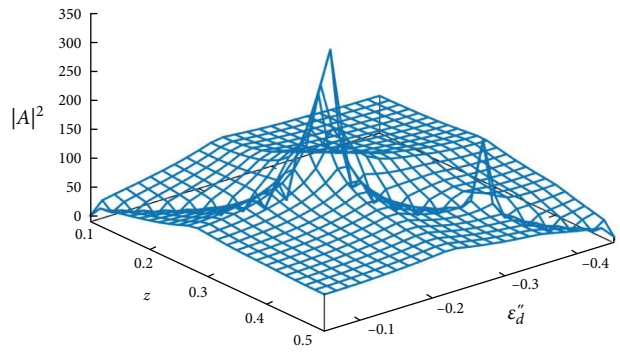

Figure 5: The local field enhancement factor $|A|^2$ for cylindrical core–shell nanoparticle versus frequency z and imaginary part of active dielectric core (ε_d'') in linear host matrix.

property of the imaginary part of the dielectric function of the dielectric core at the same dimensionless resonance frequency. This is akin to increasing the density of the cylindrical core–shell nanoparticle.

This result shows that the first maximum value of the LFE factor increased from 506 to 1,104 as the magnitude of the imaginary part of the dielectric core increased from 0.0 to 0.15. These changes occur at a fixed dimensionless frequency ($z = 0.276$). Similarly, the second maximum value of the LFE factor increased from 170 to 244 as the magnitude of the imaginary part of the dielectric core increased from 0.0 to 0.15. This variation is observed at a dimensionless frequency of $z = 0.4$. The LFE factor describes the extent to which the electromagnetic field is amplified within the nanocomposite structure compared to its surroundings. An increase in the optical density of the nanocomposite indicates that more light is confined and interacts within the structure, resulting in a stronger amplification of the electromagnetic field and thus an increase in the LFE factor. The enhancement factor is currently being studied in 2D, whereas Figure 5 is represented in 3D. The physical quantities depicted in Figures 4 and 5 were the same. However, there are distinctions between 2D and 3D graphs when utilizing an idealized active dielectric core.

Figure 6 shows that the dimensionless metal fraction (p), and the imaginary part of the dielectric core both play crucial roles in LFE by determining the resonant frequency. This result indicates that there is only one resonant frequency and one maximum value of the enhancement factor for a composite containing dielectric spherical nanoinclusions coated with metal. Modifying the dielectric properties of the core material alters the way the structure interacts with electromagnetic waves. Increasing the optical density effectively enhances the confinement of electromagnetic fields within the structure, resulting in a higher LFE factor.

3.3. Induced Optical Bistability in Cylindrical Core–Shell Nanoparticles of Passive Dielectric Core. Referring subsection (3.1), in the passive dielectric core, the natural property of the dielectric function of the dielectric core is not affected by applying additional dielectric function, then $\varepsilon_d'' = 0$. The plot

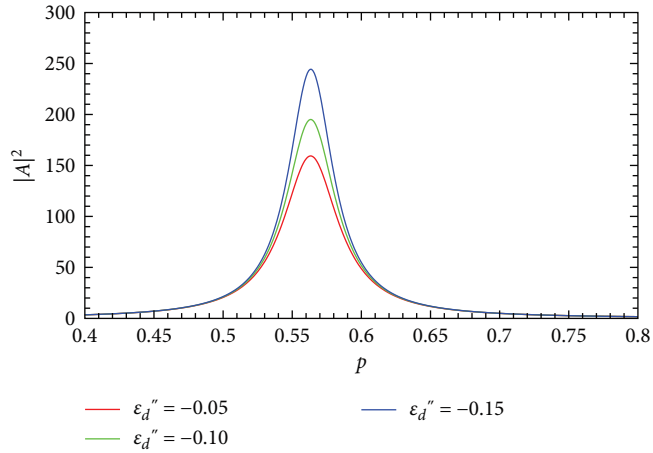

Figure 6: Enhancement factor versus metal fraction p of cylindrical core–shell nanoparticle with three different of ε_d'' at $z = 0.2$.

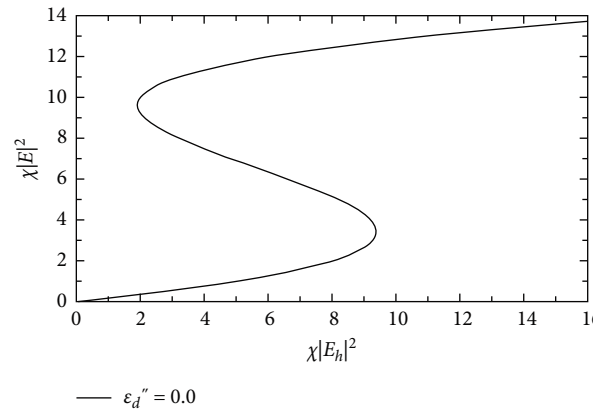

Figure 7: Induced optical bistability in nanocomposites of cylindrical shell–core in a linear host matrix for passive dielectric core ε_d'' at $z = 0.2$.

of Equation (32) for cylindrical core–shell nanocomposites in passive dielectric core is shown in Figure 7.

3.4. Induced Optical Bistability in Cylindrical Core–Shell Nanoparticles of Active Dielectric Core. In an active dielectric core, the imaginary part of the dielectric function (ε_d'') is affected by applying an additional dielectric function to it, similar to increasing the density of the cylindrical nanoparticles, resulting in $\varepsilon_d'' \neq 0$. In Figure 8, optical bistability is illustrated in the Y–X plane with observed S-like curves. The increase in $\chi|E_h|^2$ (applied field) from zero leads to a monotonic increase in $\chi|E|^2$ (local field). However, after reaching a certain value of $\chi|E_h|^2$, decreasing it results in an increase in the local field $\chi|E|^2$. Linear stability analysis indicates that this solution branch is unstable. This implies that if the system is initially in this state, it will rapidly switch to one of the stable solutions due to the growth of small perturbations. Therefore, as $\chi|E_h|^2$ increases from zero, it immediately switches to the upper branch upon passing the turning point in the lower branch. Conversely, if the input intensity is gradually decreased, the system will remain on the upper branch, and the output intensity

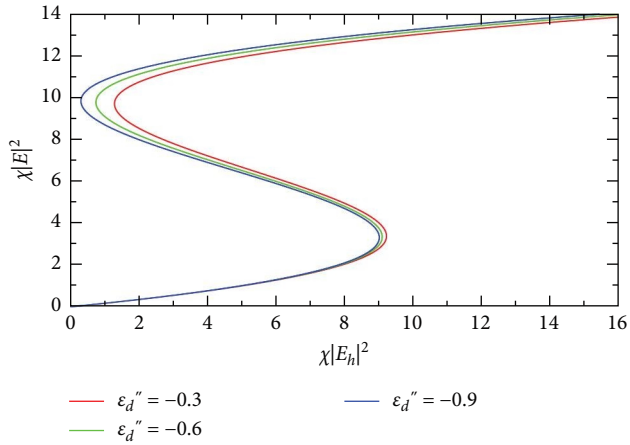

FIGURE 8: Induced optical bistability in nanocomposites of cylindrical shell–core in a linear host matrix for three different ε_d'' at $z = 0.2$.

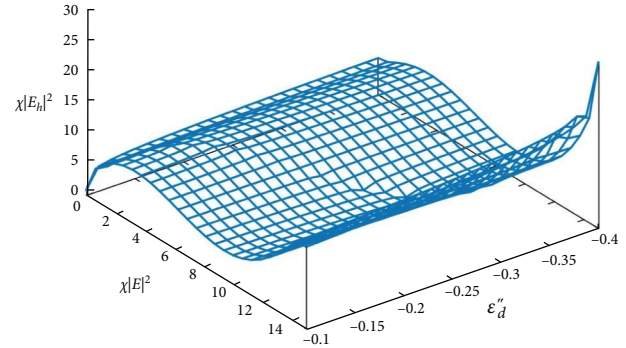

FIGURE 9: Local field ($\chi|E|^2$) versus applied field ($\chi|E_h|^2$) and imaginary part of active dielectric core (ε_d'') at frequency $z = 0.2$ in cylindrical core–shell nanoparticles that implanted in active host matrix.

will continue until it switches down to the lower branch at the turning point. In Figure 8, we observed that both the input intensities for switching up and switching down increase. However, the difference in input intensities between switching up and switching down widens as the magnitude of ε_d'' increases, leading to a broader range of optical bistability. The results indicate that the threshold for induced optical bistability increases from 7.4 to 8.7 as the magnitude of the imaginary part of the dielectric core rises from 0.0 to 0.9. This change is observed at a dimensionless frequency of $z = 0.2$. This suggests that as the magnitude of the imaginary part of the dielectric function of the core increases, the width of the optical bistability range or the threshold width broadens. This broader threshold width enhances the system's oscillation strength or increases its activation.

We chose to display a 3D graph containing these quantities to gain a basic understanding of the relationship between the applied field, local field, and the imaginary part of the active dielectric core (ε_d''). The 3D graph shown in Figure 9 was created by using Equation (32). It demonstrates this relationship within the most interesting range of these parameters, where three different values of the local field correlate to one value of the

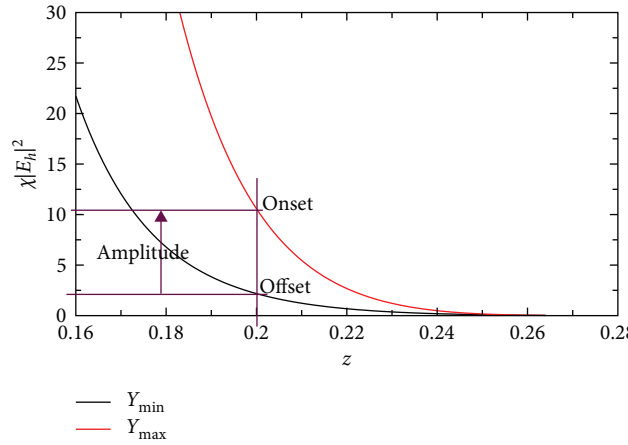

FIGURE 10: Induced optical bistability domain of the coated cylindrical nanoparticle in the plane $(z, \chi|E_h|^2)$ at $z = 0.2$ and $\varepsilon_d'' = 0.0$. The curves $Y_{\max}$ (onset) and $Y_{\min}$ (offset) are calculated with the help of Equation (34).

applied field. The bistability region, characterized by three different values of $\chi|E|^2$ for one value of $\chi|E_h|^2$, broadens as the imaginary part of the active dielectric core, ε_d'', increases.

3.5. Optical Bistability Domain in Cylindrical Core–Shell Nanoparticles. The bistability domain in the plane $(z, \chi|E_h|^2)$ can be determined through an analysis of the roots of the cubic Equation (21). There are two methods available for locating the roots of this cubic equation. The solution to Equation (21) is as follows:

$$Y = \frac{-1}{4}\left(D\left(-b \pm \frac{\sqrt{D}}{3}\right) + \frac{ab}{2}\right), \tag{34}$$

where $D = a^2 - 3b$.

In Figure 10, it is evident that the onset and offset of induced optical bistability, as described in Equation (21), correspond to the conditions outlined in the bistability domain depicted by Equation (34). The amplitude, which represents the distance between the onset and offset of induced optical bistability as shown in Figure 10, is identical to the distance between the minima and maxima of Y. This distance is calculated from the solution of the cubic equation at a specific resonance frequency, where $z = 0.2$.

Figure 11 illustrates the dependencies of the induced optical bistability domain on the imaginary part of the active dielectric core. The information extracted from the curves that enclose the bistability domain, specifically the onset and offset bistability fields at a specific dimensionless frequency, can be compared to that obtained from S-type curves. This result demonstrates that A_1, A_2, and A_3 imply an increase in the distance between the onset and offset domains of induced optical bistability with the addition of an extra dielectric function to the imaginary part of the dielectric core, specifically at ε_d'' values of 0.0, −0.3, and −0.9. The amplitudes and activation energies of the system are correlated. These findings indicate that as an additional dielectric function is

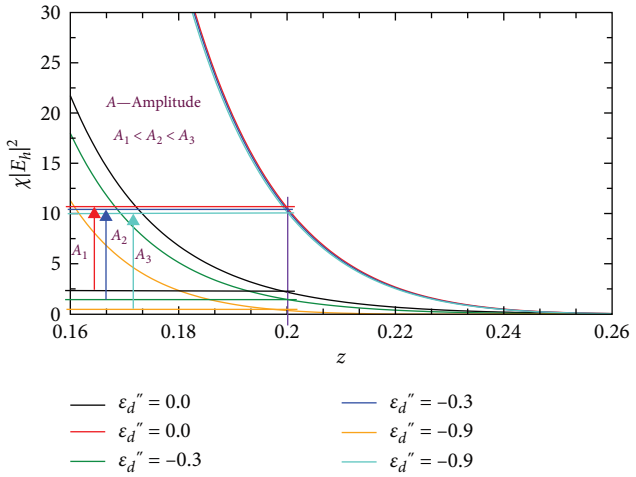

FIGURE 11: Induced optical bistability domain of the coated cylindrical nanoparticle in the plane $(z, \chi|E_h|^2)$ at $\varepsilon_d'' = 0.0$, $\varepsilon_d'' = -0.3$, $\varepsilon_d'' = -0.9$, and $z = 0.2$.

introduced to the imaginary part of the dielectric core, the domain region of induced optical bistability broadens. This suggests a potential alteration in the optical properties of the system, accompanied by a possible increase in its activation energy.

4. Summary and Conclusion

In this paper, we investigated the effect of modifying the dielectric properties of the core material in a cylindrical core–shell nanoparticle structure. Specifically, by applying an additional dielectric function to the dielectric core material, such as increasing its optical density, we observed that the LFE factor increased. This phenomenon can be explained by the interaction between the electromagnetic field and the modified dielectric core. When the optical density of the core material is increased, it alters the distribution of electromagnetic fields within the nanocomposite structure. This alteration leads to a stronger confinement and enhancement of the local electric field within the core region, resulting in an overall increase in the LFE factor. This shows that the behavior of the enhancement factor is significantly influenced by the imaginary part of the active dielectric core.

For the first maximum value of the LFE, as the magnitude of the imaginary part of the dielectric core increased from 0.0 to 0.15, the LFE increased from 506 to 1,104. This occurred at a dimensionless frequency ($z = 0.276$). For the second maximum value of the LFE, as the magnitude of the imaginary part of the dielectric core increased from 0.0 to 0.15, the LFE increased from 170 to 182. This occurred at a dimensionless frequency ($z = 0.4$). Similarly, the threshold of induced optical bistability increased from 7.4 to 8.7 as the magnitude of the imaginary part of the dielectric core increased from 0.0 to 0.9. These findings suggest that different maximum values of LFE and thresholds of induced optical bistability are influenced by variations in the magnitude of the imaginary part of the dielectric core. The research demonstrates that as the imaginary part of the dielectric function of the core increases, the range of optical bistability, or threshold width, broadens. These findings suggest that the optical bistability domain expands as the distance between switching up and switching down, or the onset and offset of optical bistability, increases.

In conclusion, this study has proposed an alternative method for enhancing the local field and increasing the threshold of induced optical bistability within cylindrical core–shell nanoparticles. By manipulating the magnitude of the imaginary part of the dielectric core at specific dimensionless frequencies, significant improvements in both LFE and the threshold of induced optical bistability were observed. These findings hold potential for advancing memory devices, optical switches, and sensor technologies.

Data Availability

This manuscript has no associated data or the data will not be deposited.

Conflicts of Interest

The author declares that there are no conflicts of interest.

Acknowledgments

I would like to thank Wolkite University for financial support.

References

[1] D. Stroud and V. E. Wood, "Decoupling approximation for the nonlinear-optical response of composite media," *Journal of the Optical Society of America B*, vol. 6, no. 4, pp. 778–786, 1989.

[2] M. F. Law, Y. Gu, and K. W. Yu, "Optical nonlinearity enhancement through correlated microstructure," *Physical Review B*, vol. 58, no. 19, pp. 12536–12539, 1998.

[3] A. K. Sarychev and V. M. Shalaev, "Electromagnetic field fluctuations and optical nonlinearities in metal–dielectric composites," *Physics Reports*, vol. 335, no. 6, pp. 275–371, 2000.

[4] S. Getachew, S. Shewamare, T. Diriba, and G. Birhanu, "Local field enhancement of cylindrical core–shell nanoparticle composites in passive and active dielectric core," *International Journal of Current Research*, vol. 15, no. 11, pp. 26432–26438, 2023.

[5] S. Arnold, T. R. O'Keeffe, K. M. Leung, L. M. Folan, T. Scalese, and A. Pluchino, "Optical bistability of an aqueous aerosol particle detected through light scattering: theory and experiment," *Applied Optics*, vol. 29, no. 24, pp. 3473–3478, 1990.

[6] R. Neuendorf, M. Quinten, and U. Kreibig, "Optical bistability of small heterogeneous clusters," *The Journal of Chemical Physics*, vol. 104, no. 16, pp. 6348–6354, 1996.

[7] J. Gea-Banacloche, W. W. Chow, and M. O. Scully, "Laser cavity dumping using optical bistability," *Optics Communications*, vol. 46, no. 1, pp. 43–46, 1983.

[8] O. A. Buryi, L. G. Grechko, V. N. Mal'nev, and S. Shewamare, "Induced optical bistability in small metal and metal coated particles with nonlinear dielectric functions," *Ukrainian Journal of Physics*, vol. 56, no. 4, pp. 311–311, 2011.

[9] A. Szöke, V. Daneu, J. Goldhar, and N. A. Kurnit, "Bistable optical element and its applications," *Applied Physics Letters*, vol. 15, no. 11, pp. 376–379, 1969.
[10] H. M. Gibbs, S. L. McCall, and T. N. C. Venkatesan, "Differential gain and bistability using a sodium-filled Fabry–Perot interferometer," *Physical Review Letters*, vol. 36, no. 19, pp. 1135–1138, 1976.
[11] V. N. Mal'nev and S. Shewamare, "Slow and fast light in metal/dielectric composites with passive and active host matrices," *Physica B: Condensed Matter*, vol. 426, pp. 52–57, 2013.
[12] G. L. Fischer, R. W. Boyd, R. J. Gehr et al., "Enhanced nonlinear optical response of composite materials," *Physical Review Letters*, vol. 74, no. 10, pp. 1871–1874, 1995.
[13] J. D. Jackson, *Classical Electrodynamics*, Wiley, New York, 3rd edn edition, 1999.
[14] Y. A. Abbo, V. N. Mal'nev, and A. A. Ismail, "Local field enhancement at the core of cylindrical nanoinclusions embedded in a linear dielectric host matrix," *Condensed Matter Physics*, vol. 19, no. 3, Article ID 33401, 2016.
[15] P. Chýlek and J. Zhan, "Absorption and scattering of light by small particles: the interference structure," *Applied Optics*, vol. 29, no. 28, pp. 3984–3984, 1990.